Journal of Applied Polymer Science

Electrolytically Exfoliated Graphene–Polylactide-Based Bioplastic with High Elastic Performance

Chakrit Sriprachuabwong,[1] Sorawit Duangsripat,[2] Komkrit Sajjaanantakul,[2] Anurat Wisitsoraat,[1] Adisorn Tuantranont[1]

[1]Nanoelectronics and MEMS Laboratory, National Electronics and Computer Technology Center, 112 Paholyothin Rd., Klong 1, Klong Luang, Pathumthani, 12120, Thailand

[2]Innophene Company Limited, 501/1 Soi Soonvijai 4, Rama 9 Rd., Huay Kwang, Bangkok, 10310 Thailand

Correspondence to: A. Tuantranont (E-mail: adisorn.tuantranont@nectec.or.th)

ABSTRACT: This work reports an innovative way to prepare biopolymer composite by incorporating graphene (GP) synthesized from electrolytic exfoliation into biodegradable polymer blend (polylactide/epoxidized palm oil: PLA/EPO) based on melt-blending method and studies their physical properties for food packaging and related applications. Multilayer GP structure synthesized by electrolytic exfoliation is confirmed by transmission electron microscopy and Raman spectroscopy, whereas homogeneous GP incorporation in PLA/EPO is verified by scanning electron microscopy and X-ray diffraction. From thermogravimetric analysis and heat deformation temperature (HDT) studies, the decomposition and HDTs of PLA/EPO/GP composites are higher than those of PLA/EPO but are lower than those of pristine PLA and tend to decrease with increasing GP content because of thermal conductivity effect. From standard tensile test, loading of GP in PLA/EPO at an optimal concentration of 0.6 wt % results in higher elongation at break by as much as 52%. The observed additional elongation under a given tension and the corresponding lower tensile strength/Young's modulus may be attributed to lower binding force of materials in the composite because of the presence of relatively weak GP–PLA/EPO interfaces. Moreover, oxygen permeability is found to decrease with increasing GP contents and oxygen permeability is reduced by 40.33% at the GP loading concentration of 0.6 wt %. © 2014 Wiley Periodicals, Inc. J. Appl. Polym. Sci. **2015**, *132*, 41439.

KEYWORDS: composites; mechanical properties; nanoparticles; nanowires; nanocrystals

Received 11 June 2014; accepted 23 August 2014

DOI: 10.1002/app.41439

INTRODUCTION

Graphene (GP), an atomically thick sheet of sp^2 carbon atoms arranged in a two-dimensional honeycomb structure, is highly promising for a wide range of applications because of its extraordinary physical, chemical, and electronic properties. In particular, GP is the strongest material with a mechanical strength (~130 GPa) over 100 times as high as steel and the highest elastic modulus (~1.0 TPa).[1] In addition, it exhibits unusually high gas permeability. GP and graphene oxide (GO) have thus been incorporated into a wide variety of materials particularly polymers to enhance their mechanical properties and gas permeability. Recent research work has demonstrated that GP-based polymer nanocomposites exhibits superior mechanical and gas barrier properties compared with pure polymer. In addition, GP offers higher property enhancement than nanoclay or other carbon filler.[2–5] For instance, Young's modulus and yield strength of polypropylene can be substantially increased up to 75% with GO loading at an optimal concentration of 0.42 wt %.[6] In addition, Young's modulus of poly(lactic acid) is improved by 18% with an addition of reduced GO at 0.2 wt %.[7] Similarly, tensile strength and Young's modulus of poly(lactic acid) (PLA) are enhanced by 15 and 85% with 0.4 wt % loadings of GP and GO, respectively, while corresponding gas permeability of composite film is found to be reduced.[8]

However, there is a pronounced tendency of agglomeration of pristine GP in polymer matrices because of strong π–π interaction of GP.[9] Therefore, an effective method to yield uniform dispersion of GP in polymer matrix is important for the development of GP–polymer composites.[10,11] GP–polymer-blend composites can be synthesized by various routes, including solution mixing, melt-blending, and *in situ* polymerization.[12] These methods involve dispersion of chemically synthesized GP powder in polymer solution, which is rather difficult. Thus, alternative GP preparation method should be used to overcome the problem. In addition to chemical synthesis through oxidation of graphite and subsequent reduction, GP may be synthesized by micromechanical cleavage, chemical vapor deposition, solvothermal

synthesis, mechanical exfoliation, epitaxial growth via ultra-high vacuum graphitization, and electrolytic exfoliation.[13] Among these, electrolytic exfoliation is a promising method for production of stable GP dispersion in an aqueous electrolyte solution because of simplicity, low cost, and ease of large-scale production.[14] It is thus a promising alternative GP synthesis method for construction of GP–polymer composites.

Bioplastics are widely developed as the potential and useful replacement of petroleum products, which cause adverse impacts on environment and will soon face serious shortage. Polylactide or PLA is an aliphatic polyester-type bioplastic, which can be chemically synthesized from monomers that can be produced from agricultural raw materials such as flour and sugar. It is commonly formed by extrusion, injection molding, and compression processes and used for packaging products such as cups, plates, and bottles. Although it can be molded by the same process of normal plastic, it tends to suffer from cracks because of brittleness and poor elastic elongation. An effective approach to this problem is blending of PLA with epoxidized palm oil (EPO), which is a suitable plasticizer of PLA because its epoxidized derivative structure of glycerol containing a variety of saturated and unsaturated fatty acids can form an interconnected network with PLA. It has been reported that PLA/EPO blend with a weight ratio of 4/1 can substantially enhance elongation at break by 210% compared with pure PLA.[15] Similarly, the addition of EPO in PLA–polycaprolactone blend at 10 wt % EPO content can significantly improve elastic elongation at break of the polymer composite.[16] In addition, the elongation at break of PLA/EPO blend is found to increase appreciably with increasing EPO loading.[17,18]

Nevertheless, the elastic performances of PLA/EPO are not sufficient for some advanced applications and should be further improved. GP should be a useful additive that can effectively improve mechanical properties of PLA/EPO. Recently, chemically synthesized GP powder has been incorporated into PLA/EPO by melt-blending method to improve the elastic performance of PLA/EPO.[19] However, this method tends to suffer from poor dispersion of GP powder in the polymer blend. In this work, a new process for GP/PLA/EPO composite production is developed by melt-blending of GP with PLA/EPO polymer to improve the elastic performance. Mechanical properties of the composite, including tensile strength, Young's modulus, and elongation at break with different GP contents, are characterized by ASTM (American Society for Testing and Materials) standard tensile test. In addition, oxygen permeability is measured gravimetrically based on the ASTM standard.

EXPERIMENTAL

Preparation of GP

GP solution was synthesized based on the electrolytic exfoliation method using an experimental setup as illustrated schematically in Figure 1.[13,14] Two graphite rods (1/4″ dia., Electron Microscopy Science) were submerged in 0.1 wt % of poly(styrenesulfonate) (Sigma-Aldrich) electrolyte solution and constant potential of 10 V was applied between them using a regulated dc power supply (Keithley 2420 Source) for 7 h to obtain stable GP dispersion. The GP was exfoliated from the positive

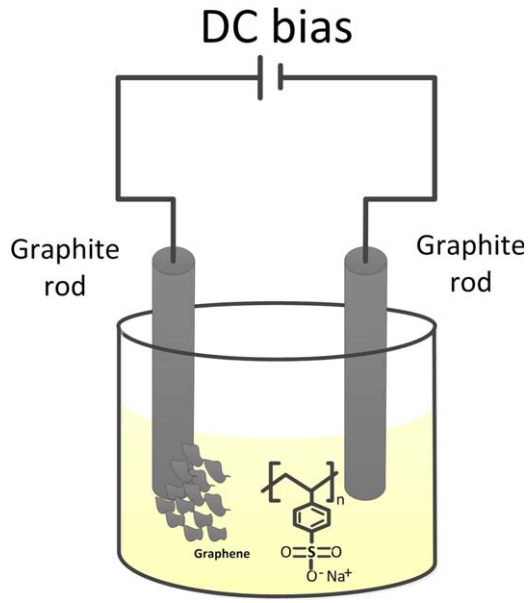

Figure 1. Schematic of graphene synthesis by electrolytic exfoliation method. [Color figure can be viewed in the online issue, which is available at wileyonlinelibrary.com.]

electrode (anode) and turns the solution into dark color with some black precipitates of agglomerated GP. Large agglomerates were separated by centrifugation at 1200 rpm and the supernatant portion was collected for the subsequent preparation of composites.

Preparation of PLA/EPO/GP Composite

PLA/EPO/GP Masterbatch was prepared by thorough mixing in a commercial internal mixer (Brabender mixer docking station, W50EHT) with rotor speed of 50 rpm at 165°C for 30 min. PLA (Commercial grade 4042D, NatureWorks) and EPO were blended at a weight ratio of 99 : 1 and poured into the Brabender internal mixer. This PLA/EPO composition was reported to yield optimal mechanical properties.[17,18] Next, the prepared supernatant GP solution was directly added with the PLA/EPO by pouring the solution into the Brabender mixer at 5–15 wt %. EPO would act as plasticizer and compatibilizer to improve the interfacial interaction between GP and PLA. The PLA/EPO/GP Masterbatch was then diluted with PLA to the desired GP concentration of 0.2–0.8 wt %. The composites were melt-blended in a twin screw extruder with a screw speed of 150 rpm at 150–190°C. Test specimens of composites were prepared according to ASTM standard for tensile test (ASTM D638) and heat deformation (ASTM D648) using injection molding machine (Battenfeld, BA250CDC).

Characterizations of PLA/EPO/GP Composite

The morphology and structure of GP dispersed in the solution were characterized by transmission electron microscope (TEM, JEOL model JEM-2010). For TEM sample preparation, GP was extracted from the solution by high-speed centrifugation at 12,000 rpm and dried in an oven at 100°C for 12 h. Dried GP powder was then dispersed in ethanol (analytical grade from RCI lab scan) with sonication and drop-coated on a standard

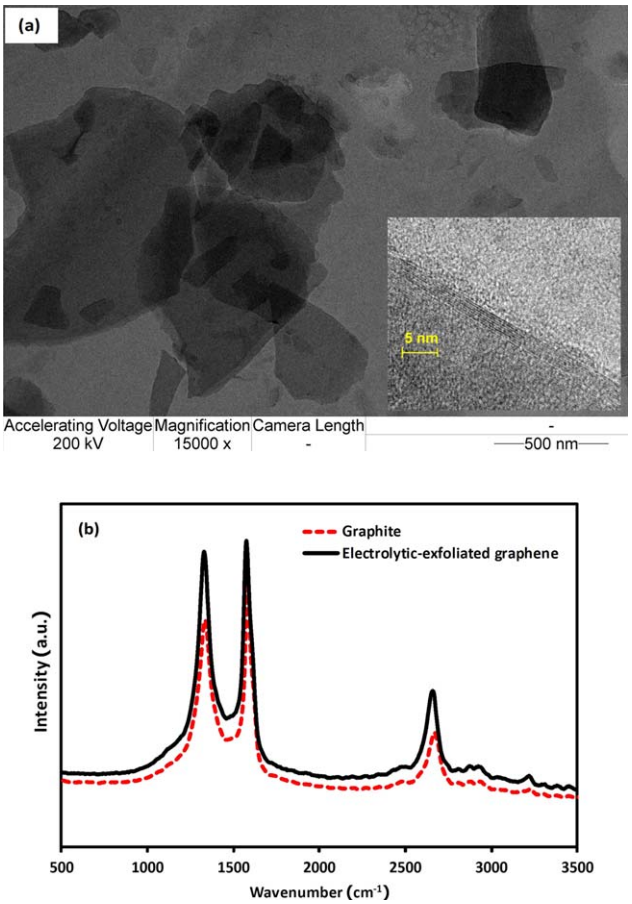

Figure 2. TEM image (a) and Raman spectrum (b) of electrolytic exfoliation graphene powder. [Color figure can be viewed in the online issue, which is available at wileyonlinelibrary.com.]

carbon/copper TEM grid. Fracture surfaces of PLA and composite after tensile test were examined by scanning electron microscope (SEM, Hitachi model S-4700). Before SEM characterization, a thin gold coating was applied to fracture surfaces of PLA and composite by a sputtering machine. Structural features of GP powder were characterized by Raman spectroscopy (NT-MDT NTEGRA). Crystal structure of PLA/EPO/GP composite was evaluated by X-ray diffraction (XRD; PANalytical X′ Pert PRO) with CuK_{α} radiation ($\lambda = 1.542$ A°) operated at 30 kV and 30 mA. Data were recorded in 2θ range of 10°–40° at the scan rate of 2°/min.

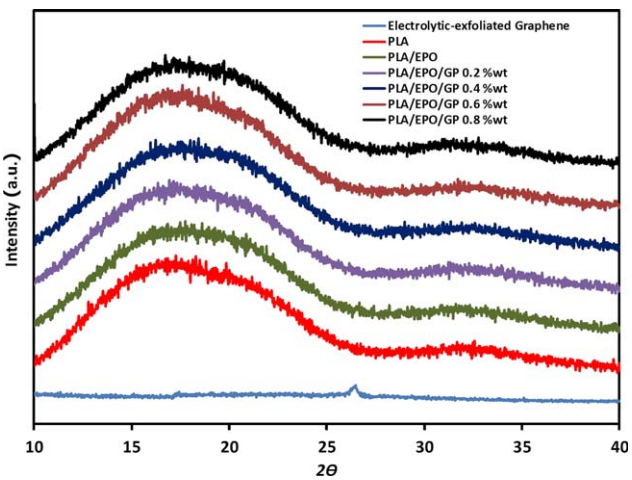

Figure 3. X-ray diffraction patterns of electrolytic exfoliation graphene powder (GP), polylactide (PLA) polylactide (PLA)/epoxy plam oil(EPO) polymer blend, and their composite with various graphene content. [Color figure can be viewed in the online issue, which is available at wileyonlinelibrary.com.]

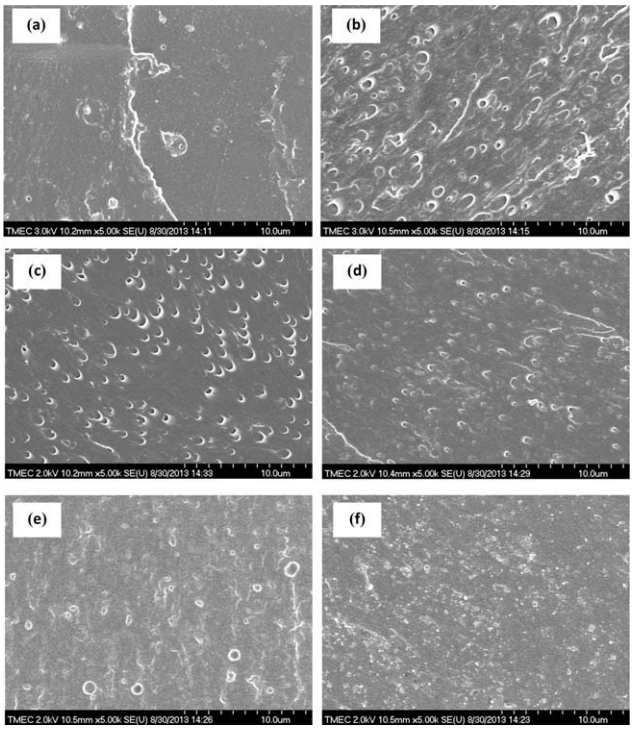

Figure 4. SEM image of fracture surface from tensile test of (a) PLA, (b) PLA/EPO, (c) PLA/EPO 0.2 wt % GP, (d) PLA/EPO 0.4 wt % GP, (e) PLA/EPO 0.6 wt % GP, and (f) PLA/EPO 0.8 wt % GP.

Thermal behaviors of PLA and composite were studied by thermogravimetric analysis (TGA) and heat deformation temperature (HDT). TGA was conducted with 5 mg of sample by thermogravimetric analyzer (Mettle Toledo TGA/STDA851e) from 50 to 500°C at 10°C/min under nitrogen atmosphere. Weight losses of samples were recorded and plotted as a function of temperature. HDTs of sample were measured using heat deformation Vicat temperature testing machine (Yasuda 148 HD) based on the standard test procedure outlined in ASTM D648.

The tensile strength, Young's modulus, and elongation at break were measured using a commercial universal tester (Instron 4302 series IX). The composite samples were injection molded into dumbbell shape following ASTM D638 standard (type V). Load of 1.0 kN was applied with a constant crosshead speed of 5 mm/min at room temperature and the stress–strain data were collected. Oxygen transmission rates of the composites were determined gravimetrically using an ASTM 1434 procedure using a commercial oxygen permeation analyzer (lllinois instruments, model 8500). The measurement was performed at 23°C and 50% relative humidity.

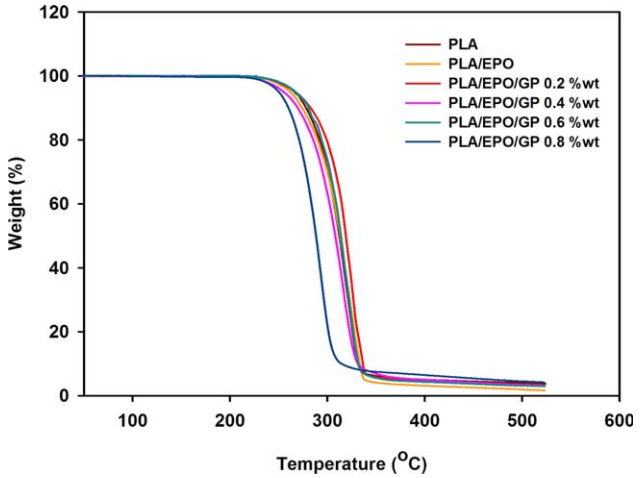

Figure 5. TGA curves of PLA, PLA/EPO, and PLA/EPO/GP composites with various graphene contents. [Color figure can be viewed in the online issue, which is available at wileyonlinelibrary.com.]

RESULTS AND DISCUSSION

Structural Characterization of GP, PLA, and Composites

Figure 2(a) shows the TEM image of GP powder dispersed in ethanol at a small concentration (1 mg/mL). It illustrates a broad distribution of large and small-size thin polygonal GP sheets around the selected area. The dimensions of these sheets are largely varied from 50 to 700 nm. High-resolution TEM as demonstrated in the inset of Figure 2(a) confirms that they are GP sheets with 6–10 layers of sp^2-bonded carbon. The corresponding Raman spectra of GP and typical graphite powder are displayed in Figure 2(b). It is seen that both Raman spectra similarly contain D, G, and 2D peaks at ~1356, ~1587, and ~2600 cm^{-1}, respectively. G and D bands are a primary in-plane sp^2 bond vibration and sp^3 non-in-plane vibrations associated with edge defects, whereas 2D peak corresponds to second overtone of non-in-plane vibrations attributed to zone boundary defects. Thus, the relatively high D/G and 2D/G intensity ratios of GP when compared with graphite indicate highly defective structural features and small sp^2 domains of electrolytically exfoliated structures.[20,21]

The XRD pattern of GP, PLA, and composite are illustrated in Figure 3. It can be seen that GP exhibits a small sharp peak at $2\theta = 26.4°$, corresponding to (002) plane of graphite lattice with a *d*-spacing of 0.34 nm, whereas PLA shows a board band at $2\theta = 16.4°$, indicating the typical amorphous structure of PLA. In addition, XRD patterns of the composites with different GP contents are nearly the same as PLA except a small peak shift at $2\theta = 17.5°$. Moreover, GP peak cannot be observed from the composite despite increasing GP content up to 0.8 wt %, which is similar to other work on GP/PLA composite.[22]

Table I. Thermal Degradation Temperature of Onset and End Weight Loss for PLA, PLA/EPO, and PLA/EPO/GP Composites with Various Graphene Contents.

Sample	Graphene content (wt %)	T_{onset} (°C)	T_{end} (°C)
PLA	—	290.7	332.0
PLA/EPO	—	294.5	329.5
PLA/EPO	0.2	302.8	336.9
PLA/EPO	0.4	286.9	328.4
PLA/EPO	0.6	295.8	332.1
PLA/EPO	0.8	267.6	304.9

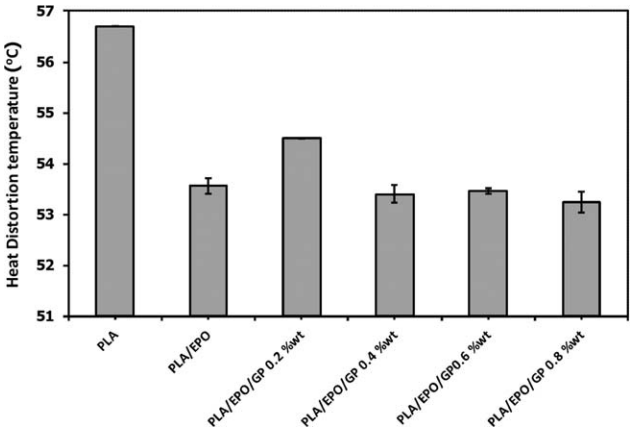

Figure 6. Heat deformation temperatures of PLA, PLA/EPO, and PLA/EPO/GP composites with various graphene contents.

SEM images displaying the characteristic fracture surface after tensile break of composites with different GP contents are shown in Figure 4. This feature is important for the strength analysis of materials. It is seen that PLA has a smooth fracture surface [Figure 4(a)], whereas PLA/EPO exhibits relatively rough texture with a number of bubble-shape and worm-like protrusions on the surface [Figure 4(b)]. For PLA/EPO/GP composites [Figure 4(c–f)], it is observed that GP concentration considerably affects the fracture surface morphology. At the

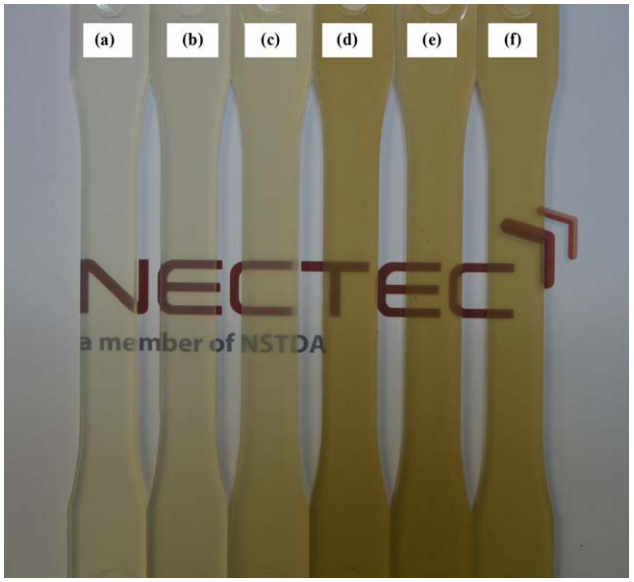

Figure 7. Tensile test specimen of (a) PLA, (b) PLA/EPO, (c) PLA/EPO 0.2 wt % GP, (d) PLA/EPO/ 0.4 wt % GP, (e) PLA/EPO/0.6 wt % GP, and (f) PLA/EPO/0.8 wt % GP. [Color figure can be viewed in the online issue, which is available at wileyonlinelibrary.com.]

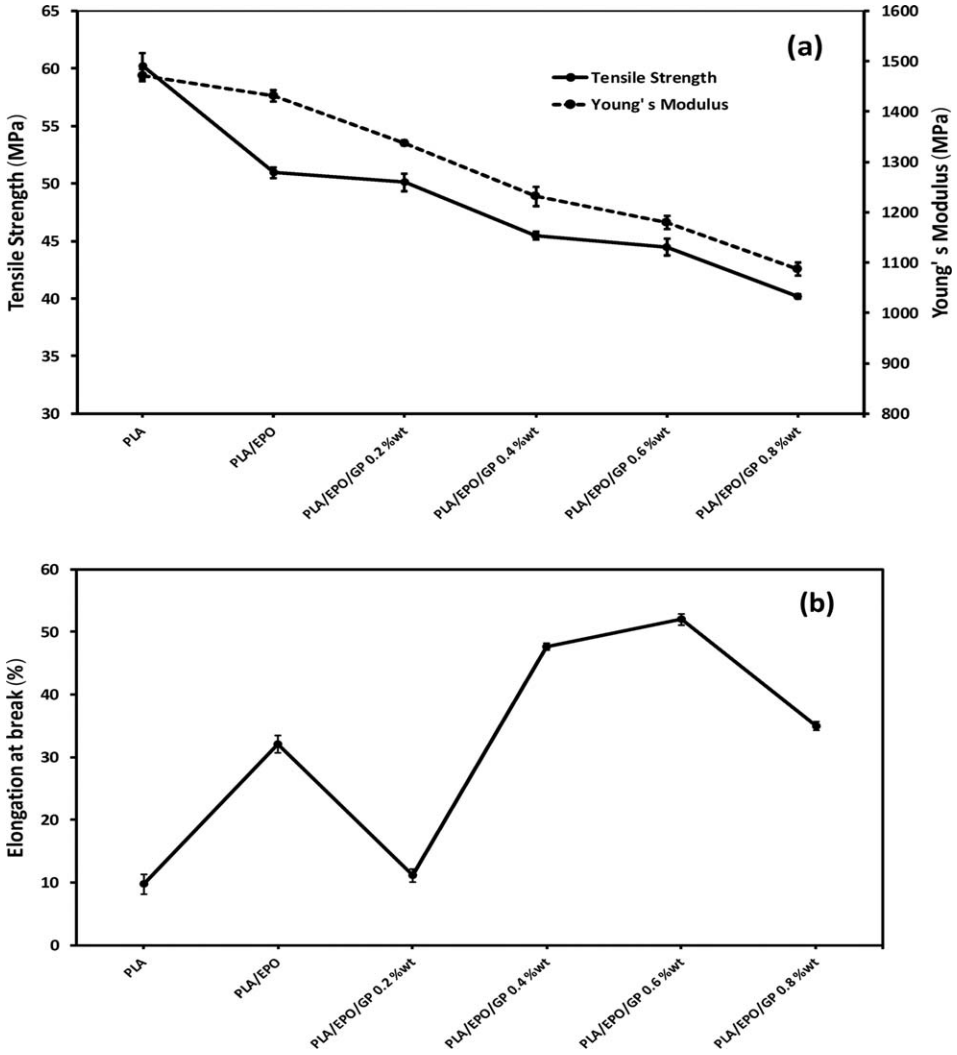

Figure 8. Tensile strength (a) and elongation at break (b) of PLA, PLA/EPO, and PLA/EPO/GP composites with various graphene contents.

lowest GP content of 0.2 wt %, the composite surface is covered with many bubble structures similar to that of PLA/EPO but with relatively smoother background surface [Figure 4(c)]. The bubble size tends to decrease with increasing GP content and the surface seems to be smoother as GP content increases [Figure 4(d–f)]. The bubbles may be the EPO phase, which is immiscible in the PLA matrix.[15,16] With increasing GP content, interaction between GP and PLA/EPO blend may lead to EPO dispersion and adsorption on GP surface, resulting in smaller EPO bubbles. It should be noted that GP sheets are occasionally found on the surface of composite, but they are not evident because of small size and smooth interface with the polymer matrix. The results indicate that GP and EPO have direct effects on strength and elongation of the PLA composite.

Thermal Analysis of PLA and Composites

Thermal stability of PLA/EPO/GP composite is evaluated by TGA at onset and the end of thermal decomposition as shown in Figure 5. Table I lists the calculated onset and ending decomposition temperature of all materials. The results indicate that thermal stability of the composites is not significantly different from those of pristine PLA and PLA/EPO. Nevertheless, it can be noticed that the thermal decomposition temperatures tend to slowly decrease with increasing GP content up to 0.6 wt %. As the GP content increases further to 0.8 wt %, the thermal decomposition temperatures decrease more significantly. From Table I, the composite with 0.2 wt % of GP has the highest onset and ending decomposition temperatures of 302.8 and 336.9°C, respectively, whereas the composite with 0.8 wt % of GP exhibits the lowest onset and ending decomposition temperatures of 267.6 and 304.9°C, respectively. The results are similar to some previous report on GP–polymer composite[23] but are in contrast to traditional 2D layered composites.[24,25] This behavior may be explained by the thermal conductivity effect.[23] High heat conductivity of GP leads to easy and rapid heat diffusion in the composites and relatively low temperature required for thermal decomposition of material. This is in accordance with the HDT results as shown in Figure 6. The HDT is measured under a given load at increased temperatures. It is seen that all composites have lower HDT than pristine PLA but relatively

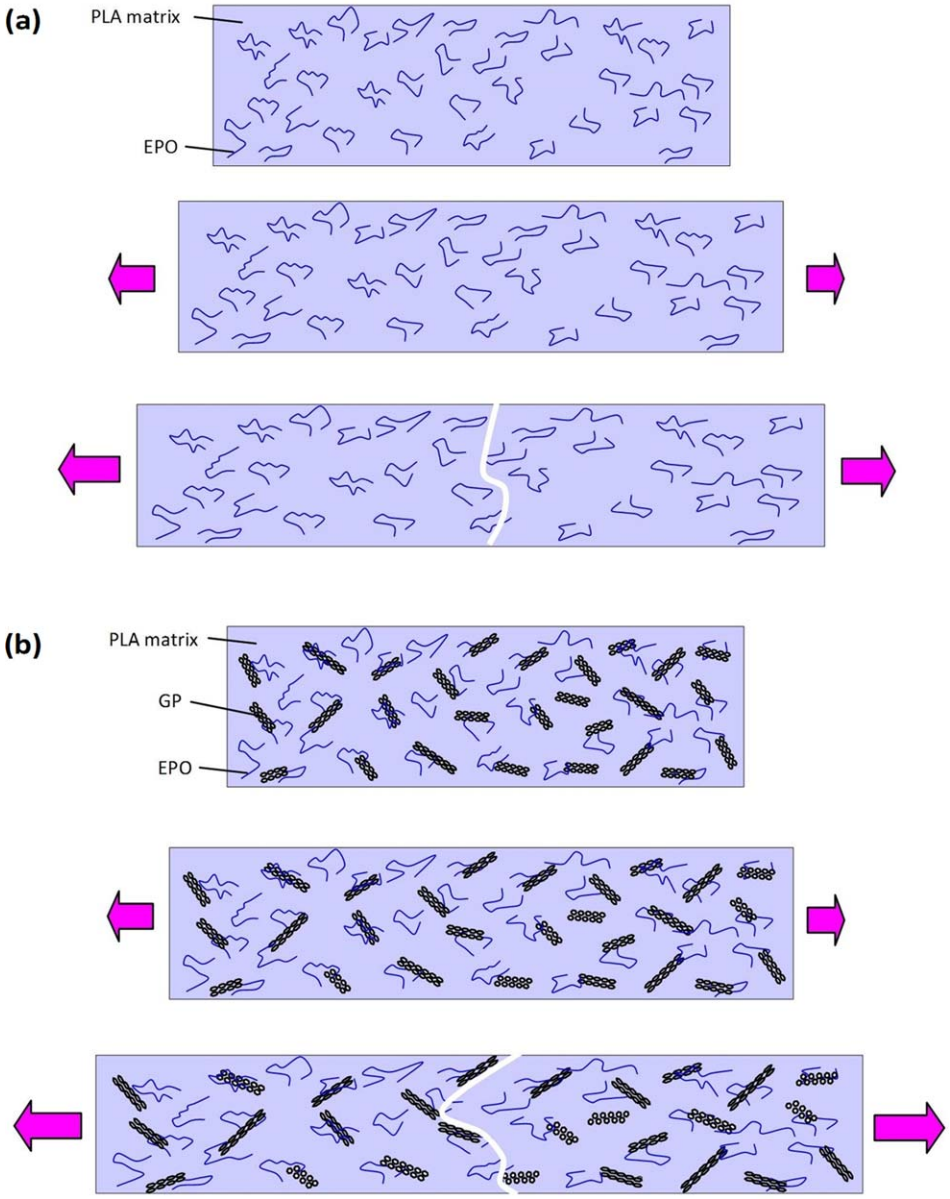

Figure 9. Physical representations of graphene in (a) PLA/EPO and (b) PLA/EPO/GP composites before elongation and after elongation until break. [Color figure can be viewed in the online issue, which is available at wileyonlinelibrary.com.]

higher or comparable with PLA/EPO. Thus, the relatively low HDT of the composites should be attributed to softening effect of EPO. In addition, the composite with the lowest GP content of 0.2 wt % has higher HDT than other composites, which is in agreement with above results on thermal stability.

Mechanical Properties of PLA and Composites

Mechanical properties of PLA and composites were evaluated by tensile test on specimens prepared based on ASTM D638 (type V) standard as shown in Figure 7. It can be seen that PLA and PLA/EPO specimens are transparent, whereas the composite specimens are increasingly dark with increasing GP content. Figure 8(a,b) shows the tensile strength/Young's modulus and elongation at break of all materials, respectively. Each data point and corresponding error bar are the average and standard deviation of the results obtained from five samples. It can be seen that the tensile strength of neat PLA is higher than those of PLA/EPO and all composites [Figure 8(a)]. In addition, tensile strength and Young's modulus of composites decrease steadily with increasing GP content. The reduction of tensile strength and Young's modulus with GP inclusion may be explained with physical representations as depicted in Figure 9. It can be seen that the presence of dispersed GP nanosheets would introduce a number of interface between GP sheets and PLA/EPO matrix, which has relatively weak interfacial adhesion. Because the tensile force is not directly applied to GP structures, the high-strength properties of GP cannot be transferred to the composite, although the presence of relatively weak GP–PLA/EPO interfaces will lead to matrix shear yielding and reduced strength.[26–30] In addition, the broad size distribution of GP

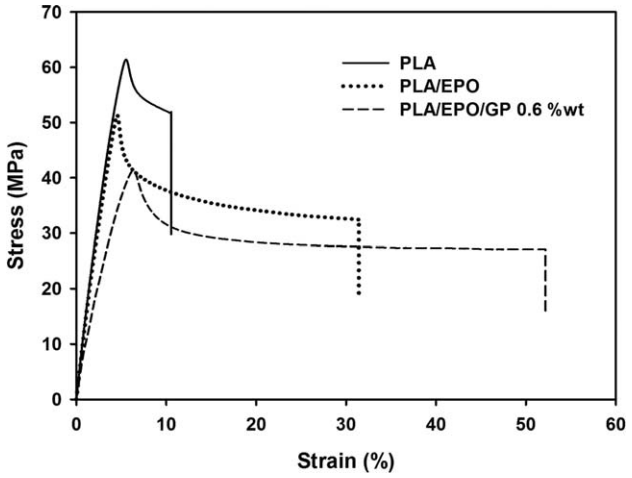

Figure 10. Stress–stain curves of PLA, PLA/EPO, and PLA/EPO/GP composites with 0.6 wt % graphene content.

sheets may lead to high connectivity of these weak interfaces, resulting in propagation of small crack into big crack and fracture of polymer nanocomposite.[30] The degraded strength performances may be improved by incorporation of nanoparticle fillers and/or plasticizers with electrolytically exfoliated GP to prevent microcrack propagation.

In contrast, the elongation at break of PLA is lower than those of PLA/EPO and most composites [Figure 8(b)]. In addition, elongation at break initially increases substantially with increasing GP content from 0.2 to 0.6 wt % but then decreases as the GP content increases further to 0.8 wt %. Moreover, stress–strain curves as shown in Figure 10 indicate that the PLA/EPO/GP composite with the optimal GP content of 0.6 wt % can have the maximum strain higher than that of PLA/EPO by as much as 52%. The improved elongation at break of PLA/EPO/GP composite may also be described with the physical representations in Figure 9. The presence of GP–PLA/EPO interfaces would provide additional elongation under a given tension because of lower binding force of materials in the composite,[15,16] and the elongation can proceed to the point where GP–PLA/EPO interfaces are disintegrated. The breaking path through GP–PLA/EPO interface could be considerably longer than that of PLA/EPO as illustrated in Figure 9. Therefore, the elongation at break of GP–PLA/EPO could be considerably higher than that of PLA/EPO. Moreover, the observed inferior elongation at break of the composite at the highest GP concentration may be due to possible aggregation of GP sheets, which leads to lower elongation at break of agglomerated GP. The improved elongation at-break performance of electrolytically exfoliated GP–PLA/EPO composite is comparable with previously reported thermally reduced GO–PLA/EPO composite that exhibited elongation at break of ~60% at a different optimal GP content of 0.3 wt %.[19] The previously reported thermally reduced GO involves chemical oxidation/thermal reduction process, which requires toxic chemicals, high temperature, and long processing time. Thus, GP prepared by electrolytic exfoliation is a promising alternative because of simplicity, no toxic chemical, and low processing temperature. In addition, the obtained result is substantially better than GO/PLA, thermally reduced GO–PLA, and graphite nanoplatelets/PLA nanocomposites, which showed much lower elongation at break of ~9%, ~4%, and ~3%, respectively.[22,31,32] The results confirm that EPO plays an important role in the enhanced elongation performance. The most plausible explanation is that EPO acts as a plasticizer that increases interfacial adhesion strength between GP and PLA.[15, 16]

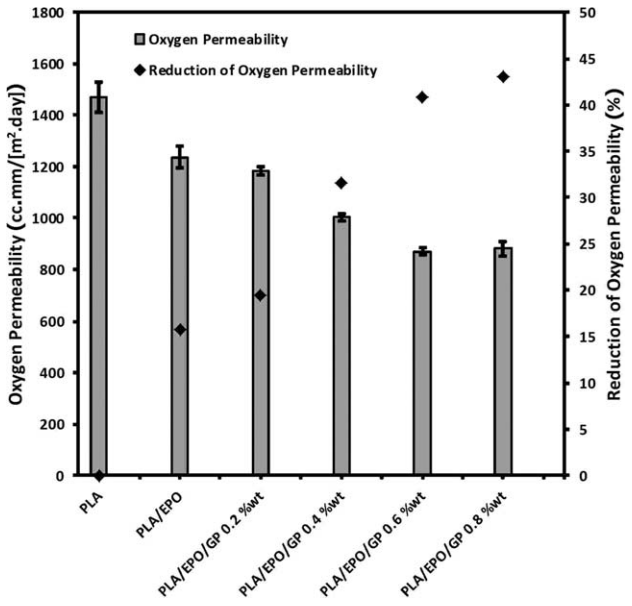

Figure 11. Oxygen permeability and reduction percentage of PLA, PLA/EPO, PLA/EPO 0.2 wt % GP, PLA/EPO/ 0.4 wt % GP, PLA/EPO/0.6 wt % GP, and PLA/EPO/0.8 wt % GP.

Oxygen Permeability of PLA and Composites

Oxygen permeability and reduction of oxygen permeability relative to PLA of all materials are given in Figure 11. It is evident that oxygen permeabilities of PLA/EPO and PLA/EPO/GP composites are lower than that of PLA. In addition, the oxygen permeability of PLA/EPO/GP composite tends to decrease with increasing GP content. The composite with 0.6 wt % GP content exhibits the lowest oxygen permeability of 869 (cc.mm/[m^2.day]) and the highest oxygen permeability reduction of 40.8%, respectively. The reduction of oxygen permeability with increasing GP content may be due to high specific surface area of GP leading to high adsorption of gas that permeates through the composite.[8] In addition, complex dispersion of exfoliated GP in polymer matrix can result in the high gas barrier property caused by tortuosity of the structure that can considerably obstruct gas permeation.[8,27–29] The low oxygen permeability of the composite is particularly useful for food packaging applications.

CONCLUSION

In conclusion, this work presents an innovative way to prepare biopolymer composite by incorporating GP synthesized from electrolytic exfoliation into biodegradable polymer blend using melt-blending method to solve GP agglomeration problem to achieve excellent GP/bioplastic composites for food packaging and related applications. TEM and Raman spectroscopy confirm that electrolytically exfoliated structures are indeed multilayer

GP. Bulk characterizations of composites by XRD and SEM indicate homogeneous dispersion of GP in the polymer blend. Thermal stability studies by TGA and HDT show that the decomposition and HDTs of the composite are higher than those of PLA/EPO but are lower than those of pristine PLA and tend to decrease with increasing GP content because of thermal conductivity effect. For mechanical properties, it was found that loading of GP in PLA/EPO at an optimal concentration of 0.6 wt % leads to higher elongation at break by as much as 52%. The observed additional elongation under a given tension and the corresponding lower tensile strength/Young's modulus may be attributed to lower binding force of materials in the composite because of the presence of relatively weak GP–PLA/EPO interfaces. Moreover, oxygen permeability is found to decrease with increasing GP contents because of increased gas adsorption by high specific surface area of GP and possibly increased tortuous effect of GP complex structure in polymer blend.

ACKNOWLEDGMENTS

This work was supported by National Electronics and Computer Technology Center (NECTEC) through graphene project under Director Initiative Program. We would like to thank Innophene Company limited for supplied graphene and pristine PLA, preparing composites by melt-blending process.

REFERENCES

1. Zhu, B. Y.; Murali, S.; Cai, W.; Li, X.; Suk, J. W.; Potts, J. R.; Ruoff, R. S. *Adv. Mater.* **2010**, *22*, 3906.
2. Layek, R. K.; Nandi, A. K. *Polymer* **2013**, *54*, 5087.
3. Kuillaa, T.; Bhadrab, S.; Yaoa, D.; Kimc, N. H.; Bosed, S.; Leea, J. H. *Prog. Polym. Sci.* **2010**, *35*, 1350.
4. Pottsa, J. R.; Dreyerb, D. R.; Bielawskib, C. W.; Ruoff, R. S. *Polymer* **2011**, *52*, 5.
5. Zhu, J.; Chen, M.; He, Q.; Shao, L.; Wei, S.; Guo, Z. *RSC Adv.* **2013**, *3*, 22790.
6. Song, P.; Cao, Z.; Cai, Y.; Zhao, L.; Fang, Z.; Fu, S. *Polymer* **2011**, *52*, 4001.
7. Cao, Y.; Feng, J.; Wu, P. *Carbon.* **2010**, *48*, 3834.
8. Artur, M. P.; Joana, C.; David, A. P. T.; Adelio, M. M.; Fernao, D. M. *Polym. Int.* **2013**, *62*, 33.
9. Stankovich, S.; Dikin, D. A.; Dommett, G. H. B.; Kohlhaas, K. M.; Zimney, E. J.; Stach, E. A.; Piner, R. D.; Nguyen, S. T.; Ruoff, R. S. *Nature* **2006**, *442*, 282.
10. Ramanathan, T.; Abdala, A. A.; Stankovich, S.; Dikin, D. A.; Herrera, A. M.; Piner, R. D.; Adamson, D. H.; Schniepp, H. C.; Chen, X.; Rodney, S. R.; Nguyen, S. T.; Aksay, I. A.; Prud, H. R. K.; Brinson, L. C. *Nature Nano* **2008**, *3*, 327.
11. Tjong, S. C. *Express Polym. Lett.* **2012**, *6*, 437.
12. Dilini, G.; Mingchao, W.; Meinan, L.; Nunzio, M.; Eric, W.; Cheng, Y. *Graphene.* **2012**, *1*, 30.
13. Guoxiu, W.; Bei, W.; Jinsoo, P.; Ying, W.; Bing, S.; Jane, Y. *Carbon.* **2009**, *47*, 3242.
14. Sriprachuabwong, C.; Karuwan, C.; Wisitsorrat, A.; Phokharatkul, D.; Lomas, T.; Sritongkham, P.; Tuantranont, A. *J. Mater. Chem.* **2012**, *2*, 5478.
15. Emad, A.; Jaffar, A. M.; Wan, M. Z. W. Y.; Nor, A. B. I.; Mohd, Z. A. *J. Mater. Sci.* **2010**, *45*, 1942.
16. Emad, A.; Jaffar, A. M.; Nor, A. B. I.; Kamyar, S.; Mansor, B. A.; Wan, M. Z. W. Y. *Res. Chem. Intermed.* **2013**, *40*, 689.
17. Giita, S.; Nor, A. I.; Wan, M. Z. W. Y.; Hazimah, A. H.; Chieng, B. W. *Int. J. Mol. Sci.* **2012**, *13*, 5878.
18. Giita, S.; Nor, A. I.; Norhazlin, Z.; Wan, M. Z. W. Y.; Hazimah, A. H. *Molecules* **2012**, *17*, 11729.
19. Buong, W. C.; Nor, A. I.; Wan, M. Z. W. Y.; Mohd, Z. H.; Giita, S. *Int. J. Mol. Sci.* **2012**, *13*, 10920.
20. Sasha, S.; Dmitriy, A. D.; Richard, D. P.; Kevin, A. P.; Alfred, K.; Yuanyuan, J.; Yue, W.; Sonbinh, T. N.; Rodney, S. R. *Carbon* **2007**, *45*, 1558.
21. Tuinstra, F.; Koenig, J. L. *J. Chem. Phys.* **1970**, *53*, 1126.
22. Il, H. K.; Youbg, G. J. *J. Polym. Sci. Part B: Polym. Phys.* **2010**, *48*, 850.
23. Chenlu, B.; Lei, S.; Weiyi, X.; Bihe, Y.; Charles, A. W.; Jianliu, H.; Yuqiang, G.; Yuan, H. *J. Mater. Chem.* **2012**, *22*, 6088.
24. Kikku, F.; Marius, M.; Giovanni, C.; Philippe, D. *Polym. Degrad. Stab.* **2010**, *95*, 1063.
25. McLauchlin, A. R.; Thomas, N. L. *Polym. Degrad. Stab.* **2009**, *94*, 868.
26. Zhao, X.; Zhang, Q.; Chen, D.; Lu, P. *Macromolecules* **2010**, *43*, 2357.
27. Hyung, C. K.; Ji, S. P.; Mi, A. J.; Hae, Y. H.; Young, T. H.; Seong, Y. H.; Sang, Y. N. *Desalination* **2008**, *233*, 201.
28. Tomomi, K.; Akira, K.; Kazukiyo, N. *Desalination* **2008**, *234*, 212.
29. Lehermeier, H. J.; Dorgan, J. R.; Way, D. *J. Membr. Sci.* **2001**, *190*, 243.
30. Zhang, X.; Alloul, O.; He, Q.; Zhu, J.; Verde, M. J.; Li, Y.; Wei, S.; Guo, Z. *Polymer* **2013**, *54*, 3594.
31. Tong, X. Z.; Song, F.; Li, M. Q.; Wang, X. L.; Chin, I. J.; Wang, Y. Z. *Comp. Sci. Tech.* **2013**, *88*, 33.
32. Li, W.; Xu, Z.; Chen, L.; Shan, M.; Tian, X.; Yang, C.; Lv, H.; Qian, X. *Chem. Eng. J.* **2014**, *237*, 291.